Available online at www.sciencedirect.com
SCIENCE DIRECT®

Journal of the European Ceramic Society 23 (2003) 2289–2295

www.elsevier.com/locate/jeurceramsoc

Synthesis and characterization of nanocrystalline $CoAl_2O_4$ spinel powder by low temperature combustion

Weidong Li*, Jiazhi Li, Jingkun Guo

Shanghai Institute of Ceramics, Chinese Academy of Sciences, Shanghai 200050, China

Received 14 August 2002; received in revised form 17 January 2003; accepted 24 January 2003

Abstract

Single-phase nanocrystalline $CoAl_2O_4$ spinel powder with a high surface area has been directly prepared by an auto-ignited gel combustion process using citric acid as a reductant/fuel and metal nitrates as oxidants. The molar ratio of fuel to nitrates in the redox mixture and the subsequent calcination upon the burnt powder were found to have a significant influence on the characteristics of the as-synthesized $CoAl_2O_4$ crystallites. By controlling the CA/NO_3^- ratio and calcination temperature, homogeneous crystalline $CoAl_2O_4$ powders with different particle sizes from 9 to 110 nm have been obtained. Gel formation, combustion behavior, microstructures and properties of the powders were characterized using DTA/TGA, FT-IR, XRD, FESEM, TEM, BET and UV/vis/IR.

Keywords: $CoAl_2O_4$; Colour; Powders-chemical preparation; Spinels

1. Introduction

Cobalt–aluminate spinel ($CoAl_2O_4$) is a thermally and chemically stable pigment of intense blue color, which has been widely used for the coloration of plastics, paint, fibers, paper, rubber, phosphor, glass, cement, glazes, ceramic bodies and porcelain enamels.[1] $CoAl_2O_4$ spinel has been conventionally synthesized using solid-state reactions which involve the mechanical mixing of various kinds of cobalt and aluminum followed by a calcination at ~1300 °C for a long period of time as well as an extended grinding. Solid-state reaction requires long-range diffusion of metal ions, which may result in inhomogeneity, larger and uneven grains (micron-sized) and poor control of stoichiometry. The unavoidable sintering caused by the high temperature calcination leads to materials with a low surface area typically of the order of 1 to 5 $m^2\ g^{-1}$.[2] The cobalt aluminate spinel by solid-state reactions which is opaque and has good hiding power is classified as ceramics-grade pigment. Since 1980s, wet-chemical techniques have been applied to prepare ultrafine $CoAl_2O_4$ spinel such as chemical co-precipitation,[3–6] sol-gel[2,7] and polymeric precursor method,[8] which has laid a good foundation for the development of the pigment-grade $CoAl_2O_4$ spinel characterized by a fine particle size and a uniform distribution. The most attractive feature of the nano-sized pigment is the transparency effects it shows along with the color generation when dispersed in a matrix. Transparency and hiding power are two contrary characteristics of a pigment, the hiding power of transparent $CoAl_2O_4$ spinel is 1/2–1/3 of that of a conventional one by solid-state reactions.[3] The special effect of transparency is very popular in plastics, paints, etc. Furthermore, $CoAl_2O_4$ Spinel by wet-chemical process has good control of stoichiometry, well-developed spinel-type structure and high purity which are in the interest of presenting a good tincting strength with a high degree of color saturation, The dispersity and dosage of the nano-sized pigment in the matrix is very important for getting a desired tincting effect and transparency.

The low temperature combustion synthesis (LCS) technique has been proved to be a novel, extremely facile, time-saving and energy-efficient route for the synthesis of urtrafine powders.[9–11] LCS is based on the

---

* Corresponding author. Tel.: +86-21-52411200; fax: +86-21-52413903.

E-mail address: liwd@mail.sic.ac.cn (W. Li).

0955-2219/03/$ - see front matter © 2003 Elsevier Ltd. All rights reserved.
doi:10.1016/S0955-2219(03)00081-5

gelling and subsequent combustion of an aqueous solution containing salts of the desired metals and some organic fuel, giving a voluminous and fluffy product with large surface area. In the present study, we report the synthesis of homogeneous nanocrystalline $CoAl_2O_4$ pigments by LCS, an auto-ignited and self-sustaining combustion of citric acid–metal nitrates gel precursor.

Table 1
Compositions of the starting solutions

Sample No.	$Co(NO_3)_2{\cdot}6H_2O$/mol	A $l(NO_3)_3{\cdot}9H_2O$/mol	Citric acid/mol	CA/NO_3^{-1}
1	1	2	1.76	0.22
2	1	2	2.22	0.28
3	1	2	2.89	0.36

2. Experimental

Analytical-grade $Co(NO_3)_2{\cdot}6H_2O$, $Al(NO_3)_3{\cdot}9H_2O$ and $C_6H_8O_7{\cdot}H_2O$ (citric acid, abbreviated as CA) were used as starting materials. An mixed solution of metal nitrates was prepared by dissolving $Co(NO_3)_2.6H_2O$ and $Al(NO_3)_3.9H_2O$ in de-ionized water with Co/Al molar ratio at 1:2. To this solution, right amounts of aqueous solution of citric acid was added in CA/NO_3^- molar ratios at 0.22, 0.28 and 0.36. The experimental compositions are listed in Table 1. Ammonia solution was slowly added to adjust the PH value at 7. The mixed solution was then heated on a hot plate with continuous agitation to evaporate excess water. As water evaporated, the solution formed a syrupy liquid, then a transparent viscous gel. The gel precursor was placed in a furnace preheated to 300 °C, and then underwent dehydration followed by decomposition resulting in deflation with the evolution of large amounts of gases, producing a dark gray foam. Afterwards the foam was automatically ignited, giving a voluminous and fluffy product of combustion. The combustion could be of the flaming type or the smouldering type depending on CA/NO_3^- ratio. The flame extinguished in only a few seconds, while the smoulder could last for more than 10 min. The type of combustion plays an important role in controlling the particle sizes of the burnt powders. The effects of CA/NO_3^- ratio on the combustion behavior of gel precursors and the characteristics of the as-synthesized powders were investigated. The burnt powders were further calcined at 500, 700, 900 and 1100 °C for 1 h to observe the microstructural development. The general flowchart for the process is shown in Fig. 1.

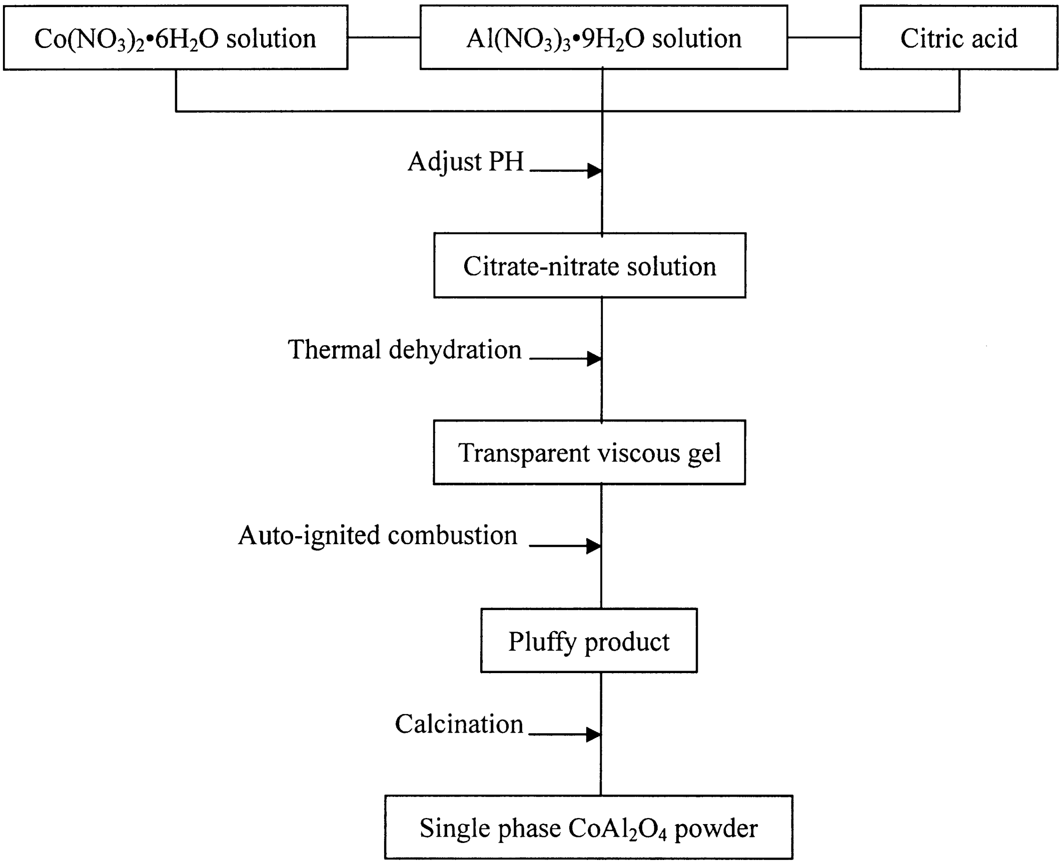

Fig. 1. Flowchart for the preparation of $CoAl_2O_4$ powder.

Thermogravimetric analysis (TGA) and differential thermal analysis (DTA) of the dried gels and the burnt powders were carried out with a thermoanalyser (STA449C, Germany) at a heating rate of 10 °C/min in static air. X-ray diffraction patterns (XRD) of the gels, the burnt and the calcined powders were recorded with an X-ray diffractometer using Cu-$K\alpha$ radiation (D/max. 2550 V, Japan). The average crystallite size was calculated employing Scherrer's equation using the profiles of the (311) peak of $CoAl_2O_4$ spinel. Infrared spectra (IR) in the range 400–4000 cm^{-1} of the gels and the burnt powders pressed with KBr were recorded using a Fourier transform infrared spectrometer (Bio-Rad FTS-185, America). The particle microstructures were investigated by a transmission electron microscope (JEM-200CX, Japan). The BET specific surface area was obtained by a micromeritics surface area analyzer (model 2400, America), using nitrogen adsorption. From the diffuse reflectance (R) spectra by a ultraviolet–visual–infrared spectrophotometer (VARIAN Cary 500, America), Kubelka–Munk absorption function $F(R)$ spectra $[F(R)=(1-R)^2/(2R)]$ were obtained to show the color characteristics of the as-synthesized $CoAl_2O_4$ powders.[12]

3. Results and discussion

3.1. Gel formation

Citric acid with one hydroxyl and three carboxyl groups is a multidentate ligand. Stable multicomponent chelates can be prepared by complexing citric acid with many multivalent ions. The as-formed gel precursors are amorphous mixtures retaining all the metallic cations in the desired stoichiometry and homogeneity, which makes it possible to prepare multicomponent oxides at temperatures much lower than using solid-state reactions.

The FT-IR spectra of citric acid, the gel precursors and the burnt powders are illustrated in Fig. 2. IR spectra for gel-1 to gel-3 are quite similar. In citric acid, the stretching vibrations for free carboxyl groups were observed between 1760 and 1700 cm^{-1}. This band splits into two bands at 1754 and 1713 cm^{-1} since citric acid has two types of carboxyl groups, one middle carboxyl group and two terminal carboxyl groups (Fig. 2a). After complexing with metal ions, two new bands occur near 1619 and 1400 cm^{-1} (Fig. 2b–d), representing the asymmetric stretching and symmetric stretching vibrations for carboxyl ions (COO^-). The difference between ν_{as} and ν_s is 219 cm^{-1}, which indicates that the carboxylate groups are coordinated to the metals in a monodentate style.[13,14] The sharp band at 1713 cm^{-1} is not found in the gels, only a very small band of free carboxyl groups near 1754 cm^{-1} can be observed in them. The bands near 1384 and 832 cm^{-1} are assigned to (NO_3^-) ions. The bands at 3140 and 3034 cm^{-1} in the gels are attributed to the stretching vibrations of the hydrogen-bonded OH groups. The earlier results indicate that Co^{2+} and Al^{3+} ions are well coordinated to the carboxylate groups. After the autoignited combustion of the gels, for $CA/NO_3^-=0.22$, no nitrate or organic residue bands are found (Fig. 2e), associated with the most intense and complete redox reaction. A small band near 1617 cm^{-1} and a small band at 1400 cm^{-1} can be observed for $CA/NO_3^-=0.28$ and 0.36 (Fig. 2f, g), showing the existence of some organic residues. New bands at 667, 559 and 417 cm^{-1} of the burnt powders indicate the formation of metal oxide, confirmed by XRD as the single-phase $CoAl_2O_4$ spinel (Fig. 5).

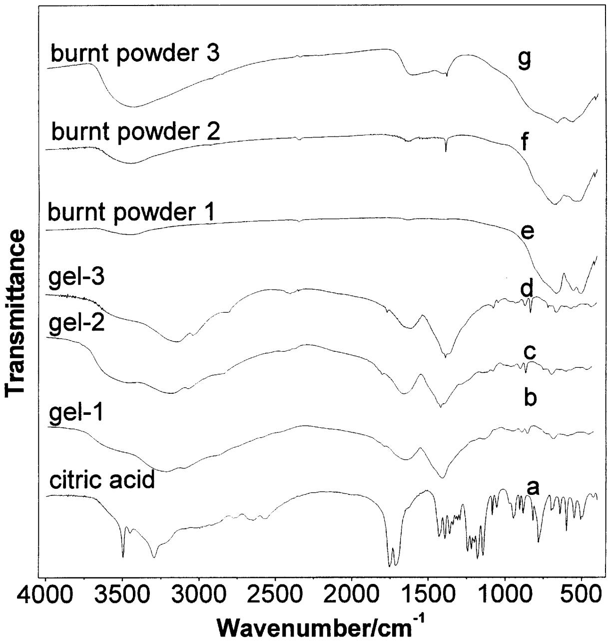

Fig. 2. FT-IR spectra of citric acid, gel precursors and burnt powders with different CA/NO_3^- ratios.

3.2. Combustion behavior

The gel precursors with different CA/NO_3^- ratios demonstrate different combustion behavior. In the reaction, metal nitrates act as oxidants and citric acid acts as a reductant/fuel. Such auto-ignited combustion of a gel precursor is a self-propagating and non-explosive exothermic reaction.

For $CA/NO_3^-=0.22$, the combustion proceeded most intensively and quickly, with flame emitting bright light, and formed bright blue pluffy foam-like product which could easily be ground to fine powder. The duration of the flame is about 10 s. Gel-1 is typified by one sharp and highly intense DTA exothermic peak at 266 °C (Fig. 3a) associated with a nearly vertical weight loss step (Fig. 3b), indicating a single temperature flash decomposition initiated by an autoignition mechanism. For $CA/NO_3^- = 0.28$, the combustion was rather moderate compared with the former one, with a weak flame lasting for about 20 s, and generated pluffy foam-like product. The foam is mainly of bright blue color tinged with dark gray, which implies that the redox reaction is not complete. The DTA curve of gel-2 (Fig. 3c) shows a sharp exothermic peak at 252 °C which is weaker than the exothermic peak of gel-1, an evidence of the main decomposition of the gel during the combustion. There is a second broad exothermic peak between 400 and 500 °C. Accordingly the TG plot of gel-2 demonstrates two weight loss steps, a nearly vertical one at 252 °C and a continuous weight loss at a lower rate up to 600 °C (Fig. 3d). For $CA/NO_3^- = 0.36$, only a faint dark red smoulder with no flame intermittently propagated through the bulk of precursor for more than 10 min, resulting in a pluffy grayish black product. The DTA curve of gel-3 (Fig. 3e) shows two distinct exothermic peaks at 260 and 440 °C with comparable intensities, related to two distinct weight loss steps (Fig. 3f). The second exothermic steps in DTA curves of gel-2 and gel-3 are presumably due to the combustion of the remaining organic residues and the oxidation of some carbonaceous residues (Fig. 3c, e).

Fig. 4 shows DTA/TG curves of the combustion-derived powders in order to further investigate the subsequent calcination process. For $CA/NO_3^- = 0.28$ (Fig. 4b), the DTA curve shows an exothermic peak at 371 °C, associated with a ~5 wt.% weight loss (Fig. 4e). For $CA/NO_3^- = 0.36$ (Fig. 4c), the exothermic peak occurs at 419 °C, corresponding to much higher weight loss of ~35 wt.% (Fig. 4f). For $CA/NO_3^- = 0.22$

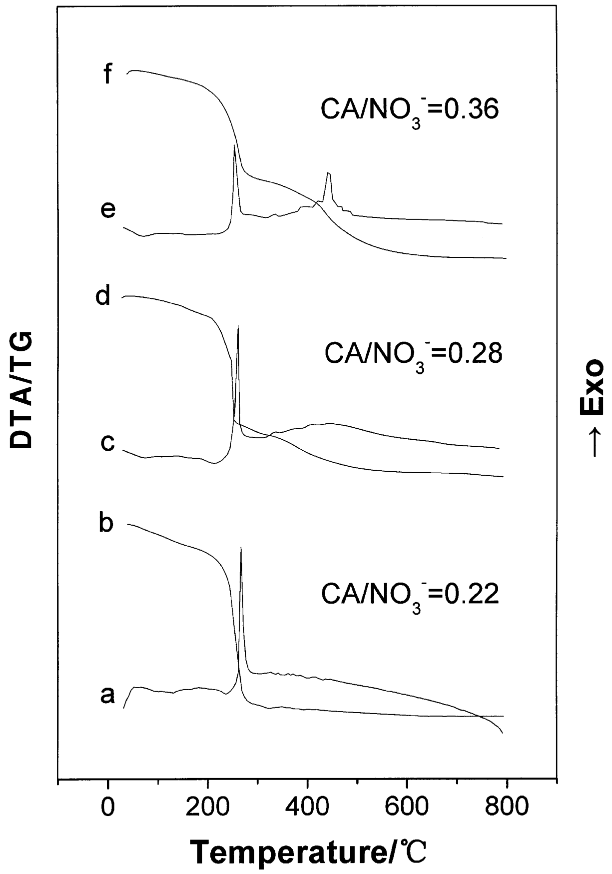

Fig. 3. DTA curves of (a) gel-1 (c) gel-2, (e) gel-3, and TG plots of (b) gel-1 (d) gel-2, (f) gel-3.

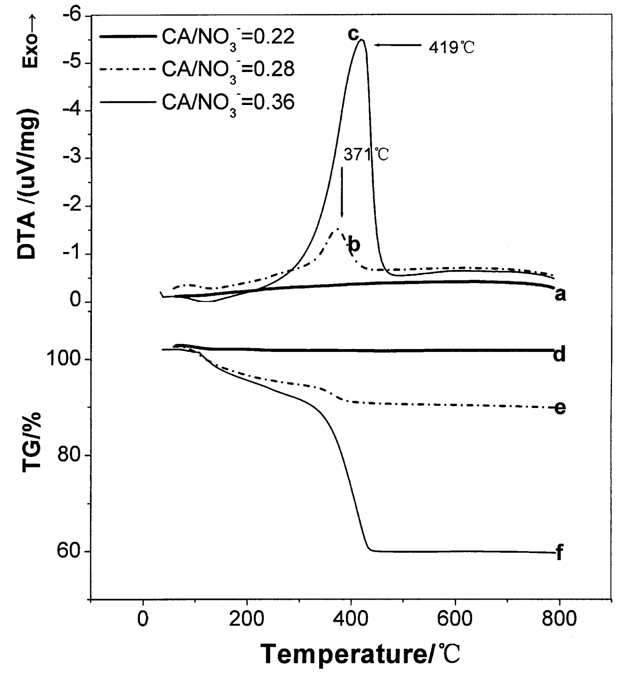

Fig. 4. DTA and TG curves of the burnt powders.

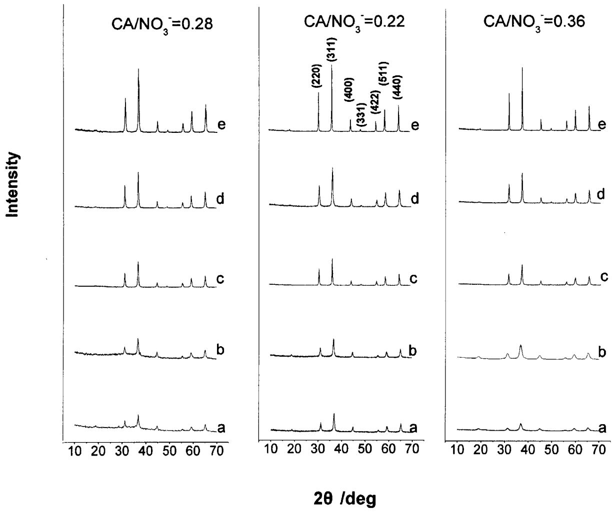

Fig. 5. XRD patterns of (a) burnt powders, and calcined powders at (b) 500 °C, (c) 700 °C, (d) 900 °C, (e) 1100 °C for 1 h, identified as single-phase $CoAl_2O_4$ spinel crystallites.

(Fig. 4a), DTA curve shows no exothermic peak, related to no weight loss (Fig. 4d), which further proves that the redox reaction is complete. It is apparent that temperature higher than 420 °C is required for organic and carbonaceous residue removal.

The smouldering combustion ($CA/NO_3^- = 0.36$) derived powder has the largest surface area of 77 $m^2\ g^{-1}$. While the flaming combustions with larger heat released by intense redox reactions result in much less residues but lower powder surface area as well, 53 and 45 $m^2\ g^{-1}$ for $CA/NO_3^- = 0.28$ and 0.22, respectively.

The stoichiometric composition of the redox mixture for the combustion synthesis can be calculated according to the concept of propellant chemistry,[15] based on the equality of total oxidizing and reducing valencies of the oxidant and the fuel for the maximum energy release. But the exact stoichiometric composition for a given system cannot be calculated unless the exact final oxidation state of nitrogen, carbon and hydrogen, as well as that of the constituent metal elements are known.[16] Obviously the hypothetic stoichiometric CA/NO_3^- ratio of 0.28 based on simply postulating the nitrogen in the combustion product as N_2 (Ref. 17) does not reflect the true stoichiometric composition in our case. In this study, the heat evolution is maximum when $CA/NO_3^- = 0.22$ with a single step exothermic reaction. For $CA/NO_3^- = 0.36$, the excess of fuel in the mixture requires some additional time to react with the ambient oxygen, maintaining the system at an elevated temperature for a relatively longer period of time, while it can be presumed that the flame temperature is the lowest one associated with the mildest exothermic reaction among the three combustions. When $CA/NO_3^- = 0.28$, the fuel is slightly rich with a small secondary exothermic peak to remove a small amount of residues.

3.3. Phase formation and morphology

XRD patterns (Fig. 5) show that crystalline cubic spinel $CoAl_2O_4$ was formed as the only phase present directly by the self-ignited combustions of all the three gel precursors, with particle sizes of 9.0, 15.6 and 19.1 nm (calculated by Scherrer's equation), respectively for $CA/NO_3^- = 0.36$, 0.28 and 0.22. The crystallite size of the burnt powders increases with the intensification of the exothermic reaction. The particle size remains constant after 1 h calcination at 500 °C, therefore calcinations at 500 °C can effectively remove the residual carbon in the three burnt powders, the elevation of XRD peaks for $CA/NO_3^- = 0.36$ and 0.28 results from the elimination of amorphous residues as confirmed in Fig. 5. The crystallites grow after being calcined at 700 °C or higher temperatures. The particle size increases with the enhancement of calcination temperature, and has a drastic lifting from 30 to 40 nm (900 °C) to 110 nm (1100 °C) (Fig. 6).

It is apparent that 0.22 is the most appropriate CA/NO_3^- ratio of fuel to oxidant for complete reaction, while the highest flame temperature brought by the most violent reaction leads to the largest primary particle size among the three starting compositions. It is suggested that a mild reaction between fuel and oxidants is necessary to produce finer crystallites at lower temperature.

Fig. 7 presents the general morphology of the burnt and calcined powders. The average particle size appears consistent with the data calculated by Scherrer's equation. The calcined powders are constituted by homogeneous nano-sized particles growing with increasing calcination temperature.

Kubelka–Munk absorption function $F(R)$ spectra of the calcined powders are shown in Fig. 8, presenting the characteristic spectrum of Co^{2+} in tetrahedral coordination, with a triple absorption peak in the visible region around 545 nm (green region), 585 nm (yellow–orange region), and 625 nm (red region), and with a multiple reflection valley around 496 and 465 nm (blue region), which gives rise to the blue color.[12] Compared with the $CoAl_2O_4$ spinel powders calcined at 900 °C, those calcined at 1100 °C bear lower absorption in the 545–625 nm region, but higher reflection in the blue region, especially a lower and broader valley in the region 425–465 nm, exhibiting bluer color hues. Regarding the 900 °C calcined powders, they display more like a sky-blue hue. The as-synthesized homogeneous and size-controllable nanocrystalline $CoAl_2O_4$ spinel pigment is expected to exhibit good transparency and tincting strength as a brilliant, lightfast and inert inorganic colouring agent in different matrices, its coloring performances will be reported later.

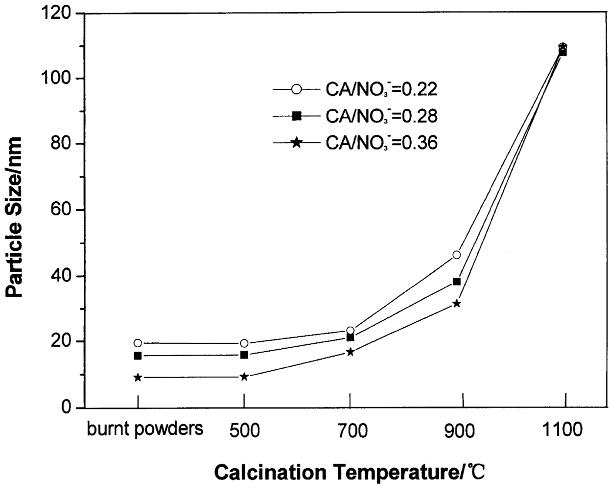

Fig. 6. Effect of calcination temperature on the particle size of $CoAl_2O_4$ crystallite.

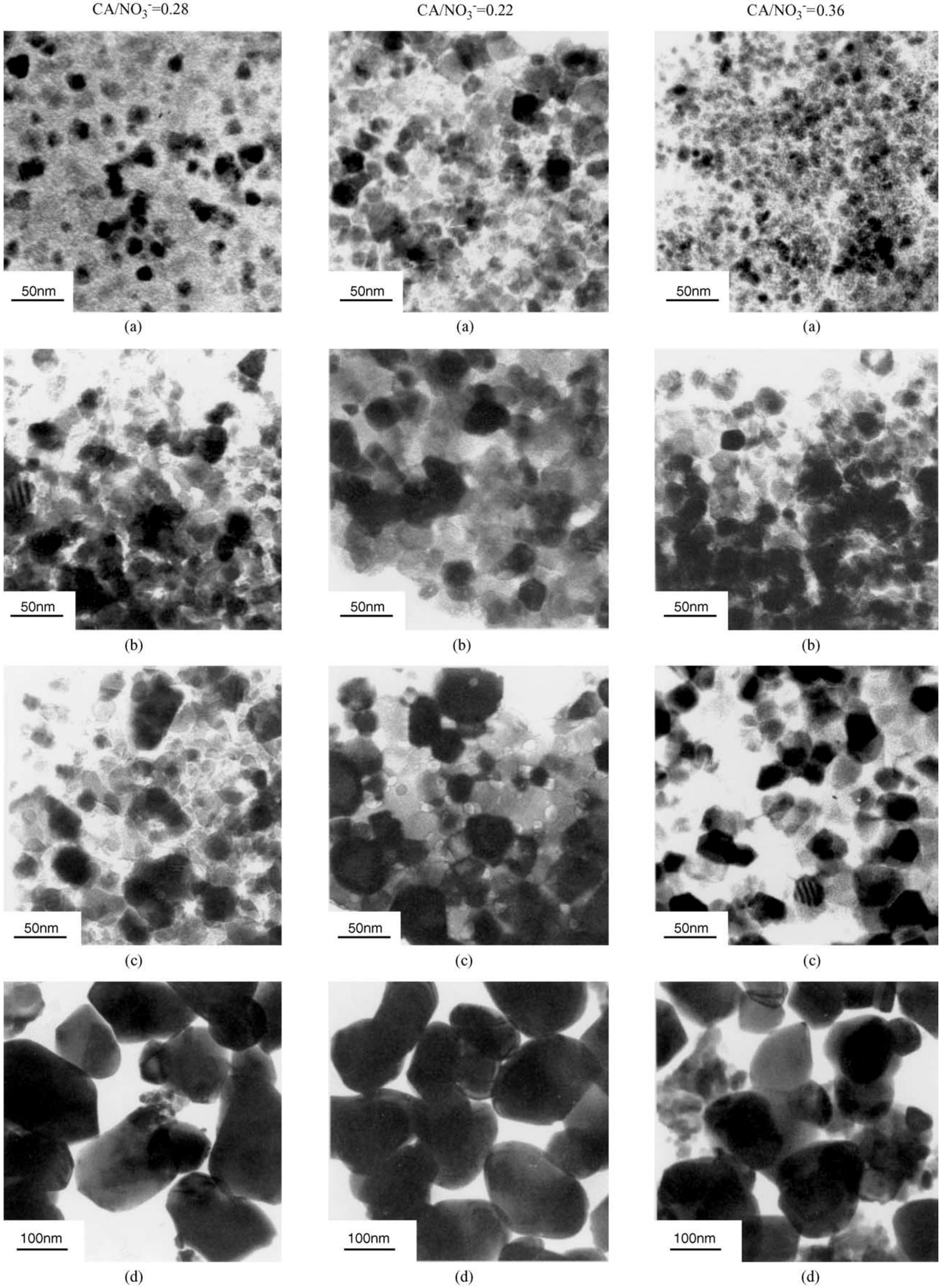

Fig. 7. TEM micrographs of (a) burnt powders, and calcined powders at (b) 700 °C, (c) 900 °C, (d) 1100 °C for 1 h.

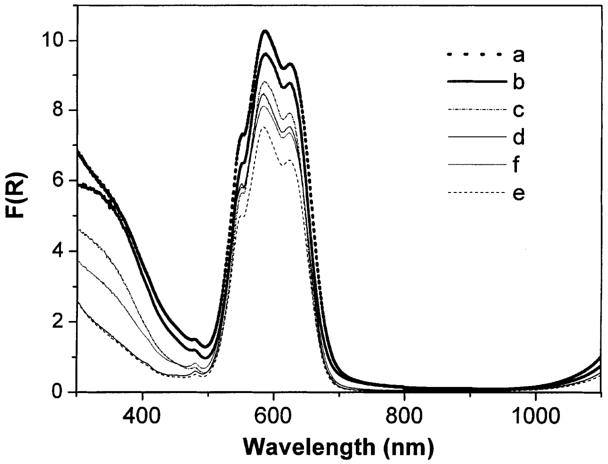

Fig. 8. Kubelka–Munk remission function spectra of the combustion derived $CoAl_2O_4$ powders. $CA/NO_3^- = 0.22$, calcined at (c) 900 °C, (d) 1100 °C for 1 h. $CA/NO_3^- = 0.28$, calcined at (b) 900 °C, (f) 1100 °C for 1 h. $CA/NO_3^- = 0.36$, calcined at (a) 900 °C, (e) 1100 °C for 1 h.

4. Conclusions

Pure and homogeneous nanocrystalline $CoAl_2O_4$ spinel powders have been directly prepared by the auto-ignited combustion of citric acid-nitrates gel precursors. The combustion products are in the form of loose agglomerates which are easily ground to fine powders. The powder characteristics are strongly dependent on the amount of heat, or the flame temperature generated by the redox reaction, which is a function of the fuel-to-oxidant ratio used in the starting composition. It is suggested that a mild reaction between fuel and oxidants is necessary to produce finer crystallites at lower temperature. The $CoAl_2O_4$ spinel particle size increases with the enhancement of calcination temperature, and has a drastic lifting from 30 to 40 nm to 110 nm when calcined at 1100 °C instead of 900 °C. The synthesized homogeneous nano-sized $CoAl_2O_4$ spinel powders display bright blue color with a triple absorption peak around 545, 585 and 625nm, and with a multiple reflection valley around 496 and 465nm.

Acknowledgements

This work was supported by the Chinese Postdoctoral Fund.

References

1. Lewis, P. A., *Pigment Handbook*, Vol. 1. John Wiley and Sons, New York, 1998.
2. Otero Areán, C., Peñarroya Mentruit, M., Escalona Platero, E., Llabrés i Xamena, F. X. and Parra, J. B., *Mater. Lett.*, 1999, **39**, 22–27.
3. Sesirô, ITô, Tadahiro, Ôkawa and Tosihide, Kuwahara, *J. Jpn. Soc. Color Mat.*, 1981, **54**, 339–343 (Japanese).
4. Japanese Patent, 4-55322, 1992.
5. Japanese Patent, 4-55323, 1992.
6. Japanese Patent, 2-283771, 1990.
7. Chemlala, S., Larbotb, A., Persinb, M., Sarrazinb, J., Sghyara, M. and Rafiqa, M., *Mater. Res. Bull.*, 2000, **35**, 2515–2523.
8. Cho, W.-S. and Kakihana, M., *J. Alloys and Compounds*, 1999, **287**, 87–90.
9. Kingsley, J. J. and Patil, K. C., *Mater. Lett.*, 1988, **6**, 427–432.
10. Kingsley, J. J., Suresh, K. and Patil, K. C., *J. Mater. Sci.*, 1990, **25**, 1305–1312.
11. Fumo, D. A., Morelli, M. R. and Segadães, A. M., *Mater. Res. Bull.*, 1996, **31**, 1243–1255.
12. Llusar, M., Forés, A., Badenes, J. A., Calbo, J., Tena, M. A. and Monrós, G., *J. Eur. Ceram. Soc.*, 2001, **21**, 1121–1130.
13. Tsay, J.-D. and Fang, T.-T., *J. Am. Ceram. Soc.*, 1999, **82**, 1409–1415.
14. Nakamoto, K., *Infrared and Raman Spectra of Inorganic and Coordination Compounds*. John Wiley, New York, 1986.
15. Jam, S. R., Adiga, K. C. and Vemeker, V. R. P., *Combust. Flame*, 1981, **40**, 71–76.
16. Zhang, Y. and Stangle, G. C., *J. Mater. Res.*, 1994, **9**, 1997–2004.
17. Purohit, R. D. and Tyagi, A. K., *J. Mater. Chem.*, 2002, **12**, 312–316.